JOURNAL OF MAGNETIC RESONANCE **134,** 255–260 (1998)
ARTICLE NO. MN981512

2D CP/MAS ^{13}C Isotropic Chemical Shift Correlation Established by ^{1}H Spin Diffusion

M. Wilhelm,* H. Feng,† U. Tracht,* and H. W. Spiess*,[1]

*Max-Planck-Institut für Polymerforschung, Postfach 3148, D-55021 Mainz, Germany, and †Wuhan Institute of Physics and Mathematics, Chinese Academy of Sciences, Wuhan 430071, People's Republic of China

Received February 27, 1998; revised May 20, 1998

A new 2D solid-state CP/MAS ^{13}C NMR exchange experiment for through-space isotropic chemical shift correlation is proposed and demonstrated. Through-space correlation is established via a second cross polarization from ^{13}C to ^{1}H and subsequent ^{1}H spin diffusion. A third cross polarization results in the final ^{13}C–^{13}C isotropic chemical shift correlation. The ^{1}H spin diffusion time is a variable parameter allowing different mean square magnetization displacements to be probed. Experimental results on mixtures of differently ^{13}C-labeled alanine and polyethylene indicate that this site-selective 2D technique can be used to characterize domain sizes and proximities over a wide range of length scales (1–200 nm) in solids such as polymers or biological materials.

Key Words: **2D ^{13}C CP/MAS NMR; ^{1}H spin diffusion; heterogeneity; spatial correlation.**

1. INTRODUCTION

Most complex materials such as polymers, composite materials, molecular sieves, minerals, and biological materials are spatially or dynamically heterogeneous. Hence, the study of heterogeneities and interfaces plays a key role in establishing the relationship between microscopic structure and macroscopic properties (*1, 2*). This knowledge is needed for further improvements in designing new materials. Among the techniques used to characterize microstructures, one- and two-dimensional solution and solid-state NMR has become an indispensable tool (*3–6*).

In solid-state NMR, especially, proton spin diffusion (*7*) is used to investigate quantitatively the length scale of spatial heterogeneities ranging from 1 to about 200 nm (*4, 5*). In this type of solid-state NMR experiment the dynamics of a non-equilibrium distribution of proton magnetization are measured while the equilibrium is restored through a diffusion process. For a known spin-diffusion constant the mean square displacement of magnetization density can be calculated. The spin-diffusion constant has been quantified experimentally in different systems (*8–17*). Usually, the selection of ^{1}H magnetization is based either on chemical shift separation or differences in spin relaxation rates (T_2) due to mobility gradients (*5, 8, 9, 12*). The classical Goldman–Shen pulse sequence (*13*) and advanced versions (*10*) are typical representatives of the latter case.

The poor spectral resolution of ^{1}H NMR detected spin diffusion prevents such techniques from being widely applied. Both the narrow chemical shift range (about 10 ppm) and the strong homonuclear dipolar interaction lead to rather featureless ^{1}H solid-state NMR spectra. Although the ^{13}C isotropic chemical shift range spans about 200 ppm and different functional groups give well-resolved peaks under CP/MAS conditions, the low natural abundance of ^{13}C severely restricts the efficiency of homonuclear ^{13}C experiments. A compromise can be reached by using ^{13}C detection of ^{1}H spin diffusion (*5*). Such an experiment takes advantage of both the fast spin diffusion among protons ($D = 0.1–1$ nm^2/ms, depending on the inherent mobility) and the high structural resolution of ^{13}C CP/MAS.

^{13}C-edited ^{1}H-spin diffusion, however, will be able to provide the necessary information only if ^{1}H selection of one phase is possible (*4, 5*). This limitation can be overcome by the novel 2D-exchange CP/MAS experiment proposed here, which uses proton spin diffusion combined with the high spectral resolution of solid-state ^{13}C CP/MAS NMR in *two* dimensions. This leads to unique site-selective information about the spatial proximity of structural elements. Several examples are presented which indicate that this pulse sequence provides unambiguous information on spatial connectivity and also on the size of the spatial heterogeneities. This new technique will be useful for determining spatial proximities within multicomponent systems such as polymer blends, copolymers, or composite materials.

2. DESCRIPTION OF THE EXPERIMENT

As is common in 2D exchange NMR (*3, 4*), the presented experiment consists of four distinct time periods; see Fig. 1 and Table 1.

(a) Preparation period. Using standard Hartmann–Hahn cross polarization (CP) (*18*), magnetization is transferred from

[1] To whom correspondence should be addressed.

1090-7807/98 $25.00

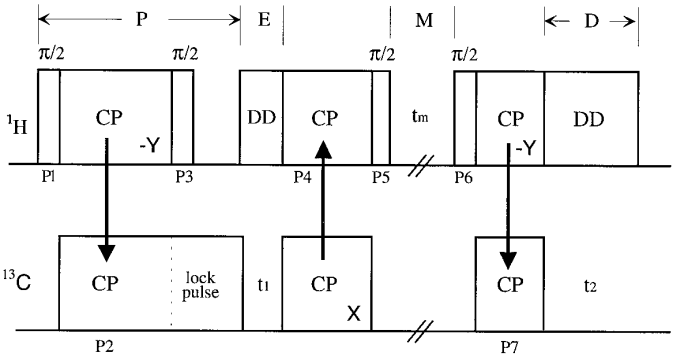

FIG. 1. Pulse sequence used for the ^{13}C 2D CP/MAS NMR experiment. This experiment correlates different carbon sites via ^{1}H spin diffusion during t_m. A detailed description of the four periods (P, preparation; E, evolution; M, mixing; and D, detection) is given in the text. The phases of the pulses P1–P7 are given in Table 1. In the experiments the CP times for P2, P4, and P7 were all set to be equal.

protons to carbons. A proton $\pi/2$ pulse is followed by a cross polarization sequence to create carbon transverse magnetization. A second proton $\pi/2$ pulse stores the remaining locked proton magnetization along $+z$. A short dephasing period eliminates residual proton transverse magnetization while the carbon magnetization remains spin locked. At the end of the preparation period ^{13}C transverse coherence has been created and the ^{1}H magnetization is stored exclusively along $+z$.

(b) Evolution period. During the evolution period t_1, the ^{13}C spins precess under the effects of chemical shift and Zeeman interactions in the presence of proton decoupling. Incrementation of the evolution period leads to high resolution ^{13}C CP/MAS spectra along ω_1.

(c) Mixing period. A second Hartmann–Hahn CP contact creates ^{1}H coherence from the ^{13}C source. The subsequent proton $\pi/2$ pulse converts the transverse coherence into longitudinal magnetization along $\pm z$. The ^{1}H magnetization migrates during the mixing time t_m by ^{1}H spin diffusion. No proton decoupling is applied to eliminate residual ^{1}H and ^{13}C transverse coherences. Hence, proton spin diffusion is limited by T_1 and not by the shorter T_2 or $T_{1\rho}$ relaxation times. The dynamics of the ^{1}H magnetization can be approximated as a diffusive process characterized by the mean square displacement $\langle r^2 \rangle$. It is in the simplest case given by

$$\langle r^2 \rangle = 6Dt_m, \qquad [1]$$

where D denotes the proton spin diffusion coefficient.

(d) Detection period. A third cross polarization process generates ^{13}C magnetization for a second time. This ^{13}C magnetization is detected under high power proton decoupling. The back-transferred magnetization is selected by an appropriate phase cycle.

The phase cycle of all pulses together with the receiver phase is listed in Table 1. The phase cycle is set to generate an amplitude modulated data set: $\cos\omega_1 t_1 \exp(i\omega_2 t_2)$.

In order to relate the advanced pulse sequence in Fig. 1 with standard spin diffusion techniques (*4, 5*), one can view the first half, P1–P5, as a selection period of ^{1}H magnetization, followed by ^{1}H–^{1}H spin diffusion during t_m and ^{13}C-edited detection. It is worth noting that the proton spin-diffusion coefficient in rigid organic solids is alike for many samples and has a typical value of about 0.6–0.8 nm^2/ms (*4, 5*).

3. EXPERIMENTAL

2D experiments were performed on a Bruker MSL 300 spectrometer (7.05 T, 75.47 MHz ^{13}C resonance frequency) with a commercial Bruker 4 mm double resonance MAS probehead. Data were acquired at room temperature. MAS rotation frequencies were about 6 kHz. Sixty-four t_1 increments with t_1 (t_2) dwell times of 32 μs (8 μs) and 400 μs (100 μs) were used for alanine and polyethylene, respectively. Measurement times for a single 2D spectrum ranged from 3 to 8 h. The minimum t_m value was set to 200 μs, and the cross polarization time to 800 μs. The acquisition was done off-resonance, and an amplitude modulated data set $\cos\omega_1 t_1 \exp(i\omega_2 t_2)$ was measured in all cases. This leads to purely absorptive spectra and places any zero frequency artifacts outside the relevant spectral region (*3, 4*).

The measured L-alanine (CH_3–$CHNH_2$–COOH) sample consisted of a mixture containing four types of L-alanine, 40% nonenriched and three identical amounts (20% each) ^{13}C-enriched at a single—but different—carbon position, e.g., carbonyl, methyl, or amino carbon. Several samples were produced by simply grinding the mixture in an agate mortar for different times to obtain heterogeneous mixtures with different particle sizes. A homogeneously mixed sample was obtained by dissolving the four types of alanine just described in distilled water and subsequently recrystallizing it. As reference, a fully ^{13}C enriched alanine specimen was measured as well.

TABLE 1
Phase Cycle Used for the Pulse Sequence Shown in Fig. 1

Pulse	Phase
P1	$+X\ +X\ -X\ -X$
P2	$+X\ -X\ -X\ +X$
P3	$-X\ -X\ +X\ +X$
P4	$+X\ +X\ +Y\ +Y\ -X\ -X\ -Y\ -Y$
P5	$+Y\ +Y\ -X\ -X\ -Y\ -Y\ +X\ +X$
P6	$+X\ +X\ +X\ +X\ +X\ +X\ +X\ +X$
	$-X\ -X\ -X\ -X\ -X\ -X\ -X\ -X$
P7	$+X\ +X\ +Y\ +Y\ -X\ -X\ -Y\ -Y$
	$+X\ +X\ +Y\ +Y\ -X\ -X\ -Y\ -Y$
Receiver	$+X\ -X\ +Y\ -Y\ -X\ +X\ -Y\ +Y$
	$-X\ +X\ -Y\ +Y\ +X\ -X\ +Y\ -Y$

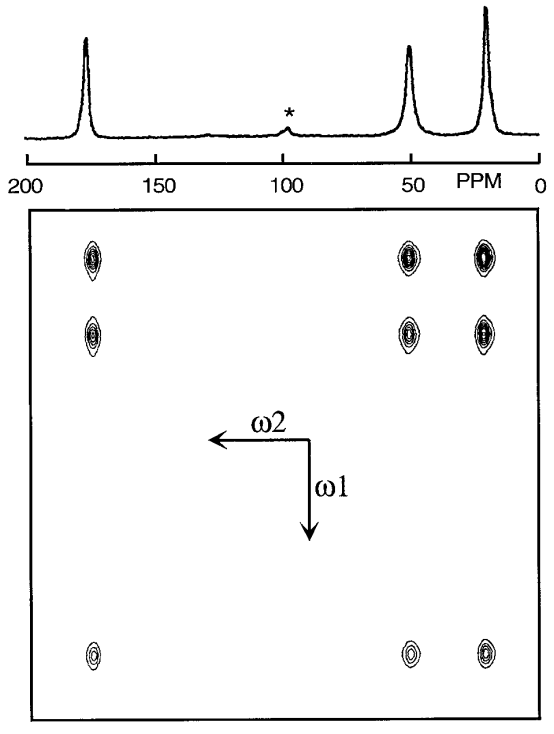

FIG. 2. 1D and 2D ^{13}C NMR spectrum of fully ^{13}C enriched L-alanine (CH_3–$CHNH_2$–COOH), t_m = 1 ms. Eight equally spaced contour levels from 7 to 95% are shown. The assignments for the alanine ^{13}C spectrum are CH_3 (20.2 ppm); CH (50.7 ppm); and COOH (178.1 ppm), with TMS as external standard. The small peak around 100 ppm marked with an asterisk is due to a spinning sideband.

Polyethylene was investigated to detect chemical shift correlation between the crystalline and amorphous phases within a semicrystalline polymer. The polyethylene sample was 4% ^{13}C labeled, with the ^{13}C labeling at two adjacent carbons (*19*).

4. RESULTS

4.1. Homogeneous Alanine Samples

Figure 2 displays the ^{13}C 2D exchange NMR spectrum of fully ^{13}C-enriched alanine recorded by application of the pulse sequence in Fig. 1 as described previously. A mixing time t_m of 1 ms was applied. All possible diagonal peaks and cross peaks are detected. The assignments for the alanine ^{13}C spectrum are CH_3 (20.2 ppm); CH (50.7 ppm) and COOH (178.1 ppm). The small peak at around 100 ppm is due to a spinning sideband of the carbonyl resonance. The cross peaks connect each carbon resonance with all other resonances. This indicates that sufficient proton spin diffusion has already occurred under those conditions. The cross peak intensities of the spectrum with 1 ms mixing time are the same as those of a spectrum with a mixing time of 200 ms (not shown).

Figure 3 displays the ^{13}C 2D spectrum (t_m = 1 ms) of an alanine sample prepared by dissolving and recrystallizing the mixture of three types of enriched alanine together with nonenriched alanine; see Section 3. As in the case of the fully enriched sample, a spin-diffusion time of only 1 ms is sufficient for all three cross peaks to appear. Changing t_m from 1 to 10 ms did not increase the intensities of the cross peaks. Thus, one can estimate that the average intermolecular distance between the differently labeled alanines is about 1 nm according to Eq. [1] using a spin-diffusion coefficient (D) of 0.6 nm^2/ms (*5*, *16*). This confirms the hypothesis that molecular mixing was achieved by the sample preparation. The reduced intensity of the cross peaks compared to Fig. 2 is due to the partial loss of magnetization caused by the larger number of protons compared to ^{13}C. It is worth noting that the 2D exchange peaks are not necessarily symmetric. The cross polarization times during P4 and P7 are equal and do not allow complete magnetization transfer for weakly dipolar coupled carbons. The transfer during P4 is reduced compared with that during P7 (*3*, *4*).

4.2. Nanoheterogeneous Alanine Sample

To test the sensitivity of this NMR method for discriminating different degrees of spatial proximities, we subsequently reduced the spatial homogeneity of a specific sample. We prepared a series of alanine mixtures with different domain sizes. This was done by grinding the previously described alanine mixture for different amounts of time.

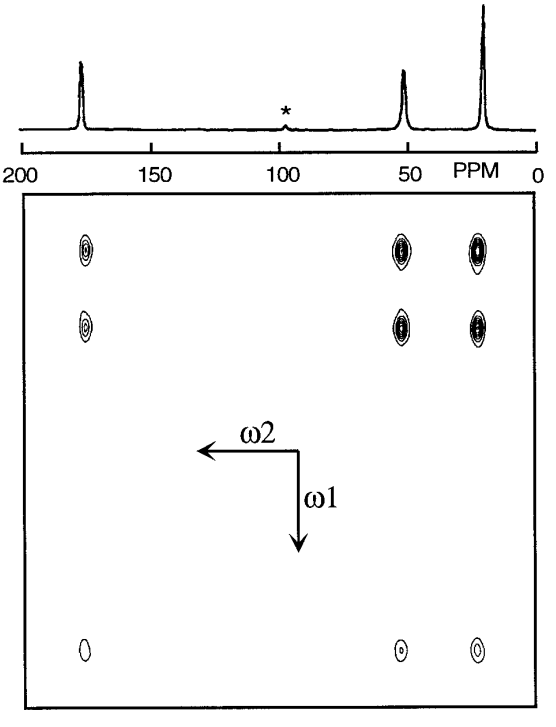

FIG. 3. ^{13}C 2D NMR spectrum of an L-alanine mixture prepared by dissolving and recrystallizing three singly ^{13}C enriched alanine samples (each 20%) together with 40% nonenriched alanine, t_m = 1 ms. Eight equally spaced contour levels from 5 to 95% are displayed.

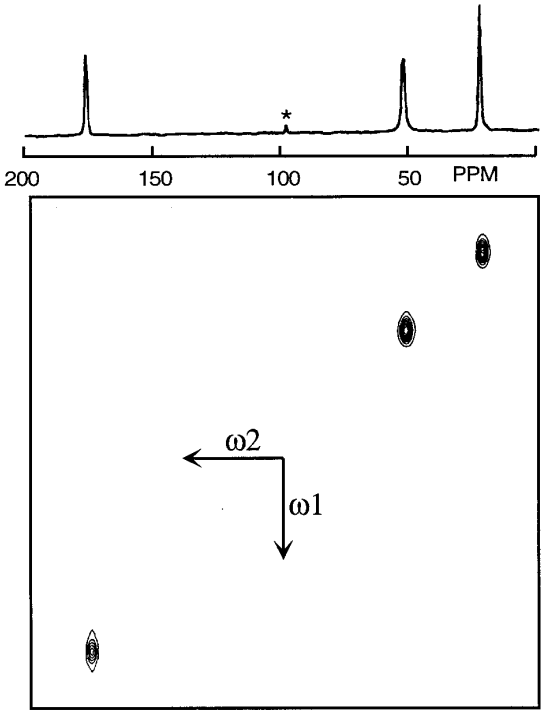

FIG. 4. ^{13}C 2D NMR spectrum of an L-alanine sample prepared by mixing the singly enriched alanine compounds. The composition of the mixture is described in the legend to Fig. 3, t_m = 200 ms. Eight equally spaced contour levels from 7 to 95% are shown.

Figure 4 displays a 2D spectrum of a sample prepared by simply mixing 20% of the three different singly enriched alanine crystals together with 40% nonenriched alanine without grinding. In the related spectrum for t_m = 200 ms only the three diagonal peaks were observed. Each diagonal peak belongs to alanine in a different environment. This confirms that in this sample the different types of alanine are macroscopically separated.

However, after the sample was subjected to grinding in a mortar for about 5 min, we obtained a different spectrum; see Fig. 5. With a spin diffusion time of t_m = 1 ms, no cross peaks could be observed in the 2D spectrum, as shown in Fig. 5a. Increasing t_m to 200 ms led to the appearance of three weak cross peaks; see Fig. 5b. Analysis of their intensities by use of Eq. [1] with D = 0.6 nm^2/ms shows that the grinding process has generated a significant number of proximities in the 20–30 nm range. To our surprise, we found that an even higher degree of intermixing can be obtained by further intense grinding (for about 30 min). In this case 1 ms mixing time was enough to obtain a 2D spectrum that contained all cross peaks as shown in Fig. 6.

4.3. Semicrystalline Polyethylene

Figure 7 displays 1D and 2D ^{13}C CP/MAS spectra of a ^{13}C-labeled polyethylene sample. The 1D spectrum contains a dominant peak at 32.3 ppm due to the high crystallinity (*20*). The broad shoulder at around 30.5 ppm reflects different conformations of amorphous segments. A mixing time of 0.5 ms leads to a mostly symmetric diagonal peak in the 2D exchange spectrum; see Fig. 7a. A considerably more extended 2D exchange pattern is detected for t_m = 16 ms; see Fig. 7b. The shape of the exchange pattern reflects the transfer of magnetization from crystalline to amorphous regions and vice versa. At this temperature and these mixing times, chain diffusion between crystalline and amorphous regions can be excluded as a cause for this (*20*). Thus, the magnetization is ascribed to proton spin diffusion. In fact, the exchange pattern of Fig. 7b can already be identified in Fig. 7a (t_m = 1 ms), yet with much lower exchange intensities. Increasing the mixing time to 32 ms had almost no effect on the intensity and shape of the exchange pattern. This indicates that the ^{1}H spin diffusion process is almost completed within the first 16 ms, as expected

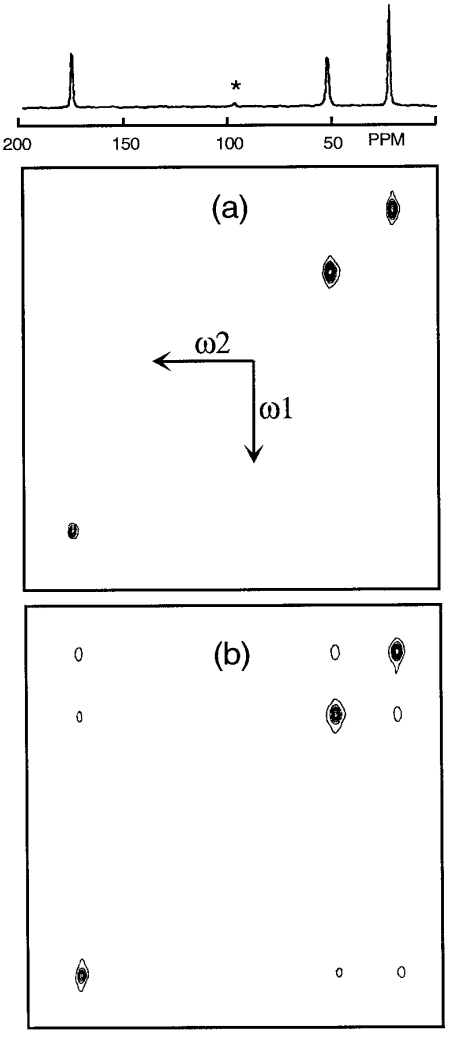

FIG. 5. ^{13}C 2D contour plots of the L-alanine sample prepared by intense grinding (5 min) of the alanine mixture leading to Fig. 4. (a) t_m = 1 ms; (b) t_m = 200 ms. Eight equally spaced contour levels, 6 to 95%, are shown.

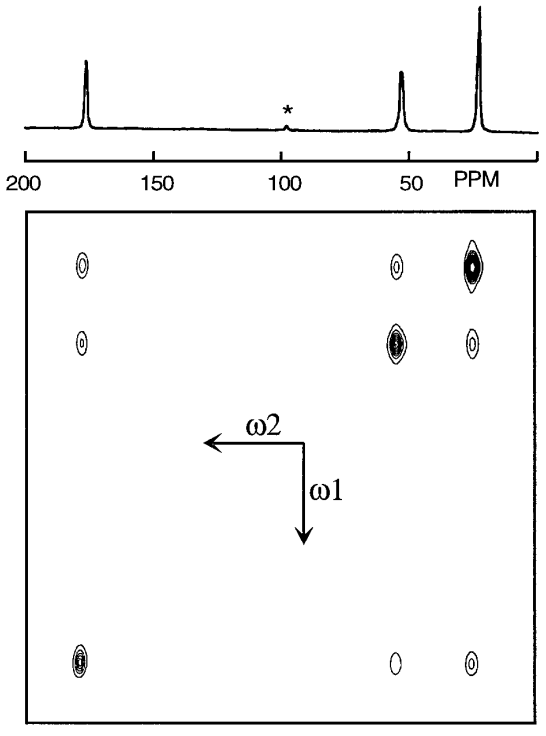

FIG. 6. ^{13}C 2D NMR spectrum of L-alanine mixture prepared by further grinding the alanine mixture (30 min) as used for Fig. 5, t_m = 1 ms. Twelve equally spaced contour levels from 3 to 85% are shown.

from the length scale of crystalline and noncrystalline regions in polyethylene known from X-ray data (*21*) to be on the order of 10 nm. It should be noted that in our sample with 4% ^{13}C enrichment in ^{13}C–^{13}C pairs, only about two such pairs are found in a crystalline stem on average. Thus, short-range magnetization exchange occurring at the interface between crystalline and amorphous regions is negligible. The 2D lineshape and also the slices through the spectrum at ω_1 = 32.3 ppm in Fig. 7b yield spectra very similar to the equilibrium 1D spectrum. Consequently, spin diffusion has equilibrated the magnetization originating from the crystalline regions within the interface and the amorphous regions.

5. DISCUSSION

The experimental examples presented in Section 4 show that our new approach can be applied not only to highly but also to moderately enriched samples. Moreover, the 2D experiment can easily be extended to a variety of related 1D and 2D versions. For example, a reduced 2D version could apply a fixed t_1 increment as a spectroscopic filter for a specific site. Another possibility is an extended 2D version in which two different types of hetero nuclei are correlated through proton spin diffusion. To resolve obvious signal/noise problems one can implement a reduced 2D version in which t_1 is set to a minimum value. This allows the selection of proton magnetization in proximity to the first hetero nucleus. Afterwards, the cross-polarized proton magnetization diffuses an adjustable distance and is finally detected at the second hetero nucleus. Utilizing proton spin diffusion can be more efficient than using or reintroducing (e.g., REDOR) direct dipolar couplings between hetero nuclei (*22–24*). This is caused by the generally much larger dipolar coupling among protons due to the smaller distances and higher magnetogyric ratio of ^{1}H.

We would also like to point out differences between the accessible length scale and spectral correlation of this method compared with liquid state NOE and INADEQUATE NMR experiments (*3, 25*), respectively. The proposed solid-state experiment can correlate carbons separated by distances as great as 1–200 nm, depending on the spin diffusion coefficient and mixing time t_m. Liquid state NOE-NMR is limited to distances within several angstroms. Nevertheless, dipolar interactions are utilized in both cases.

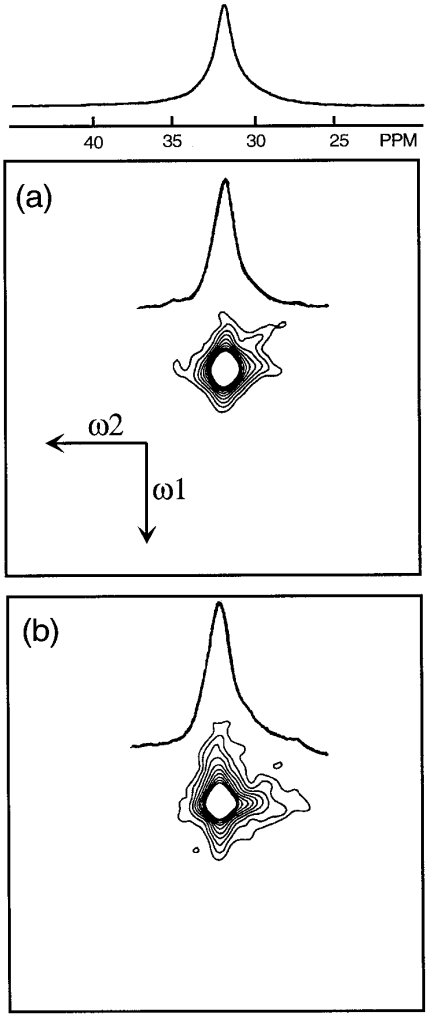

FIG. 7. ^{13}C 2D spectra of 4% ^{13}C-enriched polyethylene recorded by applying the pulse sequence of Fig. 1. (a) t_m = 0.5 ms; (b) t_m = 16 ms. Ten equally spaced contour levels from 9 to 50% are shown, together with projections and slices along ω_2.

Like the INADEQUATE technique, this new technique also establishes ^{13}C–^{13}C correlations. However, the INADEQUATE technique makes use of *J*-couplings which are only effective along covalent bonds, and consequently only connectivities to next neighboring ^{13}C are established; see also Ref. *25*. In contrast, the proposed solid-state experiment is sensitive to distances rather than bond connectivities and is not restricted to the next neighboring carbon atoms.

Likewise, the described technique extends the spatial correlation of the previously described solid-state double-quantum NMR methods of hetero nuclei (*26*). Double quantum NMR excites and correlates pairs of dipolar coupled nuclei exclusively. This strict pair correlation is in contrast to the less selective zero-quantum proton spin-diffusion process of the present sequence. Whereas solid-state double quantum NMR detects pair correlation below about 0.5 nm, the present method extends the detection of spatial correlation up to 200 nm.

6. CONCLUSION

A new 2D solid-state CP/MAS exchange NMR experiment is proposed for probing isotropic chemical shift carbon–carbon correlations. The correlation is established using proton spin diffusion during an adjustable mixing time. Experimental results on partially enriched alanine and polyethylene indicate that this technique can be used to characterize quantitatively domain sizes and proximities of a spatially heterogeneous material. The main advantages of this 2D technique are that (1) site selectivity due to high resolution of CP/MAS spectra is achieved; (2) multiple correlations among hetero nuclei can be established simultaneously; and (3) spatial correlation can be controlled within the wide range of 1 to 200 nm.

ACKNOWLEDGMENTS

HF is grateful for the financial support granted by K. C. WONG Education Foundation, Hong Kong, and the Max-Planck-Institut für Polymerforschung, Germany. UT acknowledges the financial support from the BMBF and the "Stiftung Stipendien-Fonds des Verbandes der Chemischen Industrie." We would like to thank Professor J. Zwanziger and Dr. S. De Paul for carefully checking the manuscript.

REFERENCES

1. J. M. Howe, "Interfaces in Materials," Wiley-Interscience, New York (1997).
2. J. Israelachvili, "Intermolecular and Surface Forces," Academic Press, New York (1991).
3. R. R. Ernst, G. Bodenhausen, and A. Wokaun, "Principles of Nuclear Magnetic Resonance in One and Two Dimensions," Clarendon, Oxford (1987).
4. K. Schmidt-Rohr and H. W. Spiess, "Multidimensional Solid-State NMR and Polymers," Academic Press, New York (1994).
5. J. Clauss, K. Schmidt-Rohr, and H. W. Spiess, *Acta Polym.* **44,** 1 (1993).
6. H. W. Spiess, *Ber. Bunsenges. Phys. Chem.* **101,** 153 (1997).
7. A. Abragam, "The Principles of Nuclear Magnetism," Oxford Univ. Press, London (1961).
8. P. Caravatti, P. Neuenschwander, and R. R. Ernst, *Macromolecules* **18,** 119 (1985).
9. P. Caravatti, P. Neuenschwander, and R. R. Ernst, *Macromolecules* **19,** 1889 (1986).
10. K. Schmidt-Rohr, N. Egger, D. E. Domke, B. Blümich, and H. W. Spiess, *Bull. Magn. Reson.* **11,** 418 (1989).
11. D. Suter and R. R. Ernst, *Phys. Rev. B* **32,** 4905 (1985).
12. K. Schmidt-Rohr, J. Clauss, and H. W. Spiess, *Macromolecules* **25,** 3273 (1992).
13. M. Goldman and L. Shen, *Phys. Rev.* **144,** 321 (1966).
14. T. T. P. Cheung, *J. Chem. Phys.* **76,** 1248 (1982).
15. N. M. Szeverenyi, M. J. Sullivan, and G. E. Maciel, *J. Magn. Reson.* **47,** 462 (1982).
16. D. L. VanderHart and G. B. McFadden, *Sol. State Nucl. Magn. Reson.* **7,** 45 (1996).
17. D. E. Demco, A. Johansson, and J. Tegenfeldt, *Sol. State Nucl. Magn. Reson.* **4,** 13 (1995).
18. S. R. Hartmann and E. L. Hahn, *Phys. Rev.* **128,** 2042 (1962).
19. R. Graf, D. E. Demco, J. Gottwald, S. Hafner, and H. W. Spiess, *J. Chem. Phys.* **106,** 885 (1997).
20. K. Schmidt-Rohr and H. W. Spiess, *Macromolecules* **24,** 5288 (1991).
21. L. Mandelkern, "An Introduction to Macromolecules," 2nd ed., Springer, New York (1983).
22. M. Baldus and B. H. Meier, *J. Magn. Reson.* **128,** 172 (1997).
23. T. Guillon and J. Schaefer, *in* "Advances in Magnetic Resonance," Vol. 13, pp. 57–83, Academic Press, New York (1989).
24. A. E. Bennett, R. G. Griffin, and S. Vega, *in* "NMR Basic Principles and Progress," Vol. 33, pp. 1–77, Springer, New York (1994).
25. S. Braun, H.-O. Kalinowski, and S. Berger, "100 and More Basic NMR Experiments," Wiley-VCH, New York (1996).
26. M. Feike, D. E. Demco, R. Graf, J. Gottwald, S. Hafner, and H. W. Spiess, *J. Magn. Reson. A* **122,** 214 (1996).